



HAL
open science

Deterministic models to decipher the lag phase duration during diauxie

Florian Dupeuble, Alain Rapaport, Thomas Guilmeau, Josué Tchouanti, Brice Enjalbert, Carine Bideaux, Jean-Philippe Steyer, Aida Feddaoui, Jérôme Harmand

► To cite this version:

Florian Dupeuble, Alain Rapaport, Thomas Guilmeau, Josué Tchouanti, Brice Enjalbert, et al.. Deterministic models to decipher the lag phase duration during diauxie. 10th Vienna International Conference on Mathematical Modelling (MATHMOD), Jul 2022, Vienna, Austria. pp.481-486, 10.1016/j.ifacol.2022.09.141 . hal-03610317

HAL Id: hal-03610317

<https://hal.inrae.fr/hal-03610317>

Submitted on 16 Mar 2022

HAL is a multi-disciplinary open access archive for the deposit and dissemination of scientific research documents, whether they are published or not. The documents may come from teaching and research institutions in France or abroad, or from public or private research centers.

L'archive ouverte pluridisciplinaire **HAL**, est destinée au dépôt et à la diffusion de documents scientifiques de niveau recherche, publiés ou non, émanant des établissements d'enseignement et de recherche français ou étrangers, des laboratoires publics ou privés.



Distributed under a Creative Commons Attribution - NonCommercial - NoDerivatives 4.0 International License

Deterministic models to decipher the lag phase duration during diauxie

Florian Dupeuble* Alain Rapaport** Thomas Guilmeau*
Josué Tchouanti*** Brice Enjalbert**** Carine Bideaux****
Jean Philippe Steyer* Aida Feddaoui* Jérôme Harmand*

* INRAE, Univ. Montpellier, LBE, Narbonne, France (e-mail: florian.dupeuble@insa-lyon.fr, thomas.guilmeau@ensta-paris.fr, jean-philippe.steyer@inrae.fr, jerome.harmand@inrae.fr).

** INRAE, Univ. Montpellier, MISTEA, Montpellier, France (e-mail: alain.rapaport@inrae.fr, daliyoucef.manel@gmail.com)

*** CMAP, CNRS, Ecole Polytechnique, IP Paris, 91128 Palaiseau, France (e-mail: josuetchouanti@yahoo.fr)

**** TBI, Université de Toulouse, CNRS, INRAE, INSA, Toulouse, France (e-mail: brice.enjalbert@insa-toulouse.fr)

Abstract: The deterministic model developed by Graham et al. [2020], which is the approximation in large population of a stochastic model, allowed the authors to propose a ‘macroscopic description’ of metabolic heterogeneity of *Escherichia coli* growing on glucose and xylose. However, these models did not include any mechanistic model to explain the variations of the duration of the ‘lag-phase’ observed when the glucose is exhausted and before the xylose is being consumed. Here, we propose a deterministic mechanistic model to explain how *E. coli* switches its consumption of a sugar to another one depending on the dynamic of intracellular XylR molecules. The model is developed and investigated numerically. It reveals some important observability issues.

Keywords: Diauxic growth, deterministic modeling, ODE, mass-balance models, simulation

1. INTRODUCTION

Described for the first time by Monod, the diauxic growth consists in a biphasic growth in a bacterial population consuming two different sugars in a closed medium, Monod [1942]. To study this phenomenon, a number of models have been proposed in the literature. However, a specific mechanism able to modulate the length of the lag phase as a function of its state was not proposed neither modeled and in all models the population was supposed to behave uniformly with respect to the two sugars, Turon [2015], Dedem and Moo-Young [1975], Liquori et al. [1981]. In Barthe et al. [2020], it was shown for a pure culture of *Escherichia coli* growing on glucose and xylose that ‘metabolic heterogeneity’, *i.e.* the fact that all cells do not readily switch from glucose to xylose when glucose is exhausted, could be explained by a specific internal process related to the ‘XylR transcription factor’, Song and Park [1997], Laikova et al. [2001], Schmidt et al. [2016]. This molecule is known to play a central role in the activation of the xylose pathway. In particular, depending on its history, a given cell would not contain the same number of XylR molecules than the others. The dynamic at which such a molecule would attach on a specific genomic site could explain the modulation of the duration of the lag-phases sometimes observed in the diauxic growth of this microorganism. The deterministic model developed by Graham et al. [2020], which is the approximation in large population of a stochastic model, allowed the authors to

propose a ‘macroscopic description’ of metabolic heterogeneity. However, no mechanistic modeling was proposed. Here, we propose a deterministic mechanistic model to explain how *E. coli* switches its consumption of one sugar to another depending on the dynamic of intracellular XylR molecules. The paper is organized as follows: first, the model proposed by Graham et al. [2020], hereafter called ‘macroscopic model’, is recalled together with the main modeling assumptions. Second, a deterministic mechanistic model (called the ‘compartamental model’) is presented. In a third part, simulations allowing us to provide a first analysis of the dynamical behaviours of both models are presented and used to compare their predictions. Finally, a number of modeling recommendations are suggested and discussed.

2. A MACROSCOPIC DETERMINISTIC MODEL

The model proposed by Graham et al. [2020] considered a pure culture of *E. coli* growing on two sugars, glucose (which concentration is noted s_1) and xylose (s_2). The population of bacteria is divided in two sub-populations denoted n_1 and n_2 , depending on the sugars on which they are able to grow. The sub-population n_1 can only consume glucose while n_2 preferably consumes s_1 but is also able to consume s_2 . Both sub-populations produce and consume acetate noted a . Populations n_1 and n_2 grow at rates $b_1(s_1, s_2, a)$ and $b_2(s_1, s_2, a)$, respectively. Each cell has an internal and continuous production of XylR which

accelerates in the presence of s_2 but which is inhibited by $s - 1$ due to the catabolic repression. When a XylR molecule attaches onto a specific genomic site, the xylose pathway may be ‘activated’: at this instant, the cell is no longer of type n_1 and becomes part of n_2 . The sub-population n_2 is then able to consume s_2 but under the repression of s_1 . It means that n_2 consumes s_2 under the condition that s_1 remains under a given threshold. This mechanism is modeled using a function $\eta_1(s_1, s_2)$ which is the specific rate at which n_1 converts into n_2 . Similarly, if glucose increases again in the medium, $\eta_2(s_1)$ is a function characterizing the switching rate of n_2 bacterial fraction into n_1 .

These dynamics are characterized as follows:

$$\begin{aligned}\frac{dn_1}{dt} &= (b_1(s_1, s_2, a) - \eta_1(s_1, s_2))n_1 + \eta_2(s_1)n_2 \\ \frac{dn_2}{dt} &= (b_2(s_1, s_2, a) - \eta_2(s_1))n_2 + \eta_1(s_1, s_2, a)n_1\end{aligned}$$

with $b_1(s_1, s_2, a) = \mu_1(s_1, a) + \mu_3(a)$, $b_2(s_1, s_2, a) = \mu_2(s_2, a) + \mu_3(a)$ and where $\mu_1(s_1, a) = \bar{\mu}_1 \frac{s_1}{s_1 + \kappa_1} \frac{\lambda}{\lambda + a}$, $\mu_2(s_2, a) = \bar{\mu}_2 \frac{s_2}{s_2 + \kappa_2} \frac{\lambda}{\lambda + a}$, $\mu_3(a) = \bar{\mu}_3 \frac{a}{a + \kappa_3} \frac{\lambda}{\lambda + a}$, $\eta_1(s_1, s_2) = \bar{\eta}_1 \frac{s_2}{s_2 + k_1} \frac{k_i}{k_i + s_1}$ and $\eta_2(s_1) = \bar{\eta}_2 \frac{s_1}{s_1 + k_2}$ with kinetics parameters defined as in Graham et al. [2020].

Acetate being produced by both sub-populations, and noting θ_1 and θ_2 production yields of acetate by n_1 and n_2 , and q_1 , q_2 and q_3 the yield coefficients of the biomass fractions one has:

$$\begin{cases} \frac{dn_1}{dt} = (\mu_1 + \mu_3 - \eta_1)n_1 + \eta_2 n_2 \\ \frac{dn_2}{dt} = (\mu_2 + \mu_3 - \eta_2)n_2 + \eta_1 n_1 \\ \frac{ds_1}{dt} = -\frac{\mu_1}{q_1} n_1 \\ \frac{ds_2}{dt} = -\frac{\mu_2}{q_2} n_2 \\ \frac{da}{dt} = -\frac{\mu_3}{q_3} (n_1 + n_2) + \theta_1 \mu_1 n_1 + \theta_2 \mu_2 n_2 \end{cases} \quad (1)$$

Model parameters have been identified using real data to come up with this first candidate model, *cf.* Graham et al. [2020]. Parameters values are taken from Barthe et al. [2020]. This model allows us to simulate variations of the time lag, either in changing initial conditions or model parameters. However, it remains a macroscopic model in the sense that no mechanism explicitly explains the emergence of sub-populations from an initial homogeneous species. Following the mechanistic hypothesis proposed in Barthe et al. [2020], we propose in the next section a more detailed model called the ‘Compartmental model’.

3. COMPARTMENTAL MODEL

In this section, we develop a mechanistic model of *E. coli* growing on glucose and xylose in describing specifically the dynamic of the activation of the xylose pathway via the fixation of the XylR molecule on a specific genomic site.

In terms of biomass, the model is based on the same important assumption than the macroscopic model but

both populations are further subdivided into compartments depending on the number of XylR they contain. As already mentioned, it comes from the hypothesis that the ‘transcription factor’, *i.e.* the XylR molecule, can activate the xylose pathway as soon as it is fixed on a specific genomic site allowing bacteria to consume xylose. However, it exists ‘trap sites’ (which are *xylA* promoters on plasmids) on which XylR can fix too but without giving *E. coli* the ability to consume xylose. In the following, we denote by N the number of trap sites. Accounting for the genomic site allowing the bacteria to be activated if the XylR attaches to it, the total number of sites on which XylR can fix is $n = N + 1$.

Let us note X_i the non-activated and Y_i the activated bacteria of the compartmental model. X_i contain i XylR molecules ($i = 0 \dots N$). On the opposite, Y_i contain $i + 1$ XylR molecules : i are fixed on trap sites and 1 is fixed on the promotor. For example, X_5 means that all cells within this variable contains 5 XylR fixed onto 5 trap sites, while the activated cells in the class Y_5 contain 6 XylR of which 5 are fixed onto 5 trap sites and one onto the genomic site. Likewise, X_0 is used to describe a cell containing no XylR at all, whereas Y_0 is a cell with one XylR fixed onto the ‘promotor site’.

In the macroscopic model, ‘biomass activation’ is modelled by the switching of a fraction of cells from n_1 to the compartment n_2 at a rate that depends on glucose and xylose concentrations. In the compartmental model, this passage is modeled with more details as the result of the intracellular XylR dynamic. In other words, the underlying idea is that while the lag duration is mostly the result of model parameters in the macroscopic model, it will be the result of the initial distribution of the biomass in the different compartments in the compartmental model, once its parameters will have been set once and for all.

The XylR dynamic depends on three distinct processes that are now being described.

3.1 Modelling XylR production

During a time dt , some XylR molecules are produced inside each cell. When a XylR molecule is produced, it is assumed it attaches to a site. If this site is a trap site, a cell of the class X_i quits this class and becomes a cell within the class X_{i+1} . Following the same reasoning, a cell of the class Y_i quits this class and becomes a cell within the class Y_{i+1} . Now, if the XylR attaches to the promotor site, the cell becomes activated: a cell of the class X_i quits this class and becomes a cell within the class Y_i .

At which rate does this process occur? The intracellular XylR production rate is continuous but modulated by the concentrations in glucose and xylose in the environment: it is repressed by glucose (catabolic repression occurring even at low glucose concentration) but promoted by xylose. We define $\rho_0(s_1, s_2)$ the specific production rate of XylR by one compartment as:

$$\rho_0(s_1, s_2) = \frac{k_i^4}{k_i^4 + s_1^4} \left(p_0 + \frac{\bar{\rho}_0 s_2}{k_2 + s_2} \right)$$

This function has the specific property of acting as a switching function being ‘activated’ depending on the

value of the tuning parameter k_i , and thus by a given concentration of glucose. It models a small basal production of XylR as long as s_1 is below this threshold value. The production of XylR is then further promoted as soon as there is xylose in the medium.

In Figure 1, we plotted an example of the form of ρ_0 for $k_i = 1$, $k_2 = 3$, $p_0 = 0.01$ and $\bar{\rho}_0 = 1$

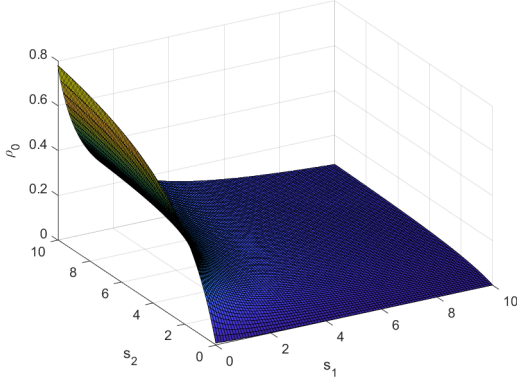


Fig. 1. ρ_0 function of s_1 and s_2

Assuming that XylR can fix on any of the trap sites or on the promotor site with the same probability, the rate at which each transition is realized is modulated by the probability to occur and the following dynamics due to the XylR production process are obtained:

$$\left\{ \begin{array}{l} \dot{X}_0 = -\rho_0 X_0 \\ \dot{X}_i = -\rho_0 X_i + \frac{N-i+1}{N-i+2} \rho_0 X_{i-1} \\ \dot{X}_N = -\rho_0 X_N + \frac{1}{2} \rho_0 X_{N-1} \\ \dot{Y}_0 = -\rho_0 Y_0 + \frac{1}{N+1} \rho_0 X_0 \\ \dot{Y}_i = -\rho_0 Y_i + \frac{1}{N-i+1} \rho_0 X_i + \rho_0 Y_{i-1} \\ \dot{Y}_N = \rho_0 X_N + \rho_0 Y_{N-1} \end{array} \right.$$

3.2 XylR degradation

Once attached to a site, it is hypothesized that a XylR molecule can degrade and detach. We define the specific degradation rate $\alpha(s_1)$ similar to $\eta_2(s_1)$.

$$\alpha(s_1) = \bar{\alpha} \frac{s_1}{k_3 + s_1}$$

Following the same reasoning as in the previous section, this rate is modulated by the probability of such process to happen. And thus, we come up with the following dynamics:

$$\left\{ \begin{array}{l} \dot{X}_0 = \alpha Y_0 + \alpha X_1 \\ \dot{X}_i = \frac{1}{i+1} \alpha Y_i + \alpha X_{i+1} - \alpha X_i \\ \dot{X}_N = \frac{1}{N+1} \alpha Y_N - \alpha X_N \\ \dot{Y}_0 = \frac{1}{2} \alpha Y_1 - \alpha Y_0 \\ \dot{Y}_i = \frac{i+1}{i+2} \alpha Y_{i+1} - \alpha Y_i \\ \dot{Y}_N = -\alpha Y_N \end{array} \right.$$

3.3 Cell division

The last process considered is the fate of the XylR molecules during cell division. In such a case, we distinguish between two different situations.

- If the cell is in a state where the production of XylR is sufficiently high (thus for cells growing on xylose), postulating that a cell divides into two exactly identical cells, it is assumed that it gives birth to two cells containing the same number of XylR. To sum up, Y_i , when growing on xylose (but not on acetate) will always divide in two new Y_i .
- If the cell is growing on glucose or acetate, the production of XylR molecules is slowed down: it does not allow the production of two identical daughters and it is assumed that the two cells produced share the number of XylR of the mother. However, how modeling the way the number of XylR are shared between the two daughters? Several modeling possibilities were hypothesized and it was finally chosen that the daughter cells shared half-half of the XylR. This dynamic is making more complex with odd i : in this case, one daughter cell will receive $\frac{i+1}{2}$ XylR proteins and the other one $\frac{i-1}{2}$.
- In addition, we assume that during division, X_i (resp. Y_i) can only produce X_i (resp. Y_i).

To model the transition from a compartment to another one for the cell division process, we use a matrix M of dimension $n \times n$ that we multiply by the vector $X = (X_0, \dots, X_i, \dots, X_N)$ or the vector $Y = (Y_0, \dots, Y_i, \dots, Y_N)$. Note that the dimensions of the matrix M depends on N . Let us first define a M_{div} matrix (of the same size as M), which is the new population of cells after a division without taking into account the mother cells disappearance. For $j \in [1, n]$: $M_{div \frac{j}{2}; j} = 1$ and $M_{div \frac{j}{2}+1; j} = 1$ for j even and $M_{div \frac{j-1}{2}+1; j} = 2$ for j odd and M_{div} equals 0 everywhere else. The terms $M_{div \frac{j}{2}; i} = 1$ and $M_{div \frac{j}{2}+1; i} = 1$ correspond to the $(i+1)$ compartment with odd number of XylR dividing half into the $\frac{j}{2}$ and half the $\frac{j}{2} + 1$ compartments. The $M_{\frac{i-1}{2}+1; i}$ correspond to the $(i+1)$ compartment with integer number of XylR dividing into the $\frac{i-1}{2}$ compartment.

M is used to characterize the total variation of the population due to cell division. To obtain it, we have to subtract the population after division to the population before division in computing $M = M_{div} - I_n$.

Supposing the growth rates are identical to those of the macroscopic model, we have:

$$\begin{cases} \dot{X}_i = (\mu_1 + \mu_3)(MX)_i \\ \dot{Y}_i = \mu_3(MY)_i + \mu_2 Y_i \end{cases}$$

3.4 Sugar dynamics

The evolution of glucose and xylose, noted s_1 and s_2 as in the macroscopic model, and the evolution of acetate are the same as in the previous model. With $\tilde{X} = \sum_{i=0}^N X_i$ and $\tilde{Y} = \sum_{i=0}^N Y_i$, it gives:

$$\begin{aligned} \dot{s}_1 &= -\frac{1}{q_1} \mu_1 \tilde{X} \\ \dot{s}_2 &= -\frac{1}{q_2} \mu_2 \tilde{Y} \\ \dot{a} &= -\frac{1}{q_3} \mu_3 (\tilde{X} + \tilde{Y}) + \theta_1 \mu_1 \tilde{X} s_1 + \theta_2 \mu_2^{act} s_2 \tilde{Y} \end{aligned}$$

3.5 Model dynamics

Adding the different components of the dynamic, we finally have:

$$\left\{ \begin{aligned} \dot{X}_0 &= (\mu_1 + \mu_3)(X_0 + X_1) + \alpha Y_0 + \alpha X_1 \\ &\quad - \rho_0 X_0 \\ \dot{X}_i &= (\mu_1 + \mu_3)(MX)_i + \frac{1}{i+1} \alpha Y_i + \alpha X_{i+1} \\ &\quad - \alpha X_i - \rho_0 X_i + \frac{N-i+1}{N-i+2} \rho_0 X_{i-1} \\ \dot{X}_N &= (\mu_1 + \mu_3)(MX)_N + \frac{1}{n} \alpha Y_N - \alpha X_N \\ &\quad - \rho_0 X_N + \frac{1}{2} \rho_0 X_{N-1} \\ \dot{Y}_0 &= \mu_3(MY)_0 + \mu_2 Y_0 + \frac{1}{2} \alpha Y_1 - \alpha Y_0 \\ &\quad - \rho_0 Y_0 + \frac{1}{N+1} \rho_0 X_i \\ \dot{Y}_i &= \mu_3(MY)_i + \mu_2 Y_i + \frac{i+1}{i+2} \alpha Y_{i+1} - \alpha Y_i \\ &\quad - \rho_0 Y_i + \frac{1}{N-i+1} \rho_0 X_i + \rho_0 Y_{i-1} \\ \dot{Y}_N &= \mu_3(MY)_N + \mu_2 Y_N - \alpha Y_N + \rho_0 X_N + \rho_0 Y_{N-1} \\ \dot{s}_1 &= -\frac{1}{q_1} \mu_1 \tilde{X} \\ \dot{s}_2 &= -\frac{1}{q_2} \mu_2 \tilde{Y} \\ \dot{a} &= -\frac{1}{q_3} \mu_3 (\tilde{X} + \tilde{Y}) + \theta_2 \mu_2 s_2 \tilde{Y} + \theta_1 \mu_1 \tilde{X} s_1 \end{aligned} \right. \quad (2)$$

4. SIMULATIONS

In this section, we perform a number of simulations in order to compare predictions of both models. Parameters used for the different simulations are taken from Barthe et al. [2020].

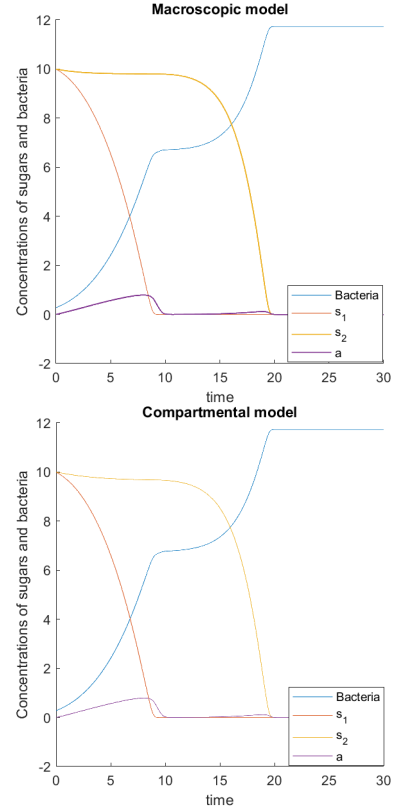


Fig. 2. Trajectories of the macroscopic (top) and of the compartmental (down) model. Initial condition : $n_1(0) = \tilde{X}(0) = 0.28 \times 0.75$, $n_2(0) = \tilde{Y}(0) = 0.28 \times 0.25$, $s_1 = 10(g.L^{-1})$, $s_2 = 10(g.L^{-1})$, $a = 0$. Time in hours.

As already mentioned, changing the distribution of the initial biomass in the compartmental model is related to control the lag duration. In other words, we would like to explain and predict the differences of lag durations using the compartmental model by the initial distribution of XylR in the population while it directly depends on model parameters in the macroscopic model.

First, we compare both models using numerical simulations for ‘equivalent’ initial conditions (*i.e.* the same proportion of active/non-active bacteria and quantities of sugar). The initial conditions in sugar concentrations and in biomass are thus equal: in the compartmental model, uniform initial conditions are chosen. For $n_1(0) = \tilde{X}(0) = 0.28 \times 0.75$, $n_2(0) = \tilde{Y}(0) = 0.28 \times 0.25$, we measured a lag of 1.85 h for the macroscopic model and 1.51 h for the compartmental model (see Figure (2)). For $n_1(0) = \tilde{X}(0) = 0.28 \times 0.25$, $n_2(0) = \tilde{Y}(0) = 0.28 \times 0.75$, we observed time lags of 1.51 h and 1.16 h, respectively (see Figure (3)). Notice that decreasing the proportion of initial active bacteria increases the lag.

Now, another objective is to be able to better understand how the initial conditions of the compartmental model allows to ‘control the lag’. Said otherwise, the question is to ‘link’ initial conditions of the compartmental model (initial biomass distribution) with the fractions of activated/inactivated biomasses of the macroscopic model. To do so, we proceed as follows:

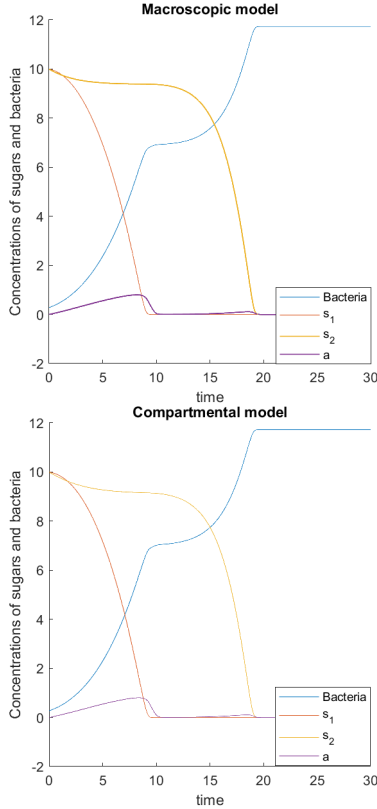


Fig. 3. Trajectories of the macroscopic (top) and of the compartmental (down) model. Initial condition : $n_1(0) = \tilde{X}(0) = 0.28 \times 0.25$, $n_2(0) = \tilde{Y}(0) = 0.28 \times 0.75$, $s_1 = 10(g.L^{-1})$, $s_2 = 10(g.L^{-1})$, $a = 0$. Time in hours.

- For a given fraction of initial biomass $n_1(0)$ and $n_2(0)$, we generate biomass and sugar profiles using the macroscopic model. We call these profiles ‘reference profile’ in the following;
- We identify some initial conditions for the compartmental model using an optimization approach that allows us to reproduce as well as possible the reference profile. To do so we used a least squared method.

We did this work for the initial conditions given by $n_1(0) = \tilde{X}(0) = 0.28 \times 0.75$, $n_2(0) = \tilde{Y}(0) = 0.28 \times 0.25$, $s_1(0) = s_2(0) = 10$. Repeating the previous described optimization procedure from initial conditions of the biomass distribution of the compartmental model (the degrees of freedom of the optimization) allowed us to highlight a very important property of the compartmental model, that is the fact that it is not observable. Indeed, in Figure 4, we plotted 20 optimized biomass distributions allowing the compartmental model to reproduce with a comparable and acceptable accuracy the trajectories of the macroscopic model departing from different sets of initial conditions. Since many sets of initial conditions predict the same trajectories of the sugar and of the total biomass, the system is probably not observable.

The first idea to deal with the unobservability of the compartmental model is to restrict the class of initial conditions in which we search for the solution of the optimization problem. Indeed, looking for the results of the optimization step within a given distribution reduces the

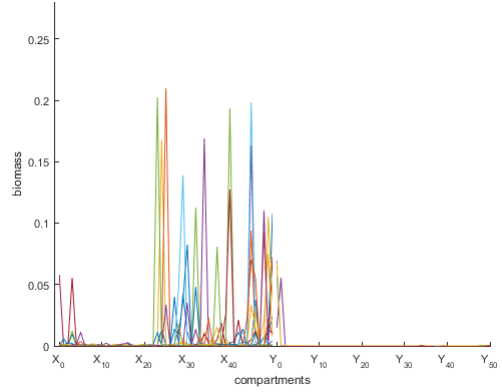


Fig. 4. Initial distributions obtained after using the least squared method on trajectories of total biomass and quantities of sugar, for $n_1 = \tilde{X} = 0.28 \times 0.75$, $n_2 = \tilde{Y} = 0.28 \times 0.25$, $s_1 = 10(g.L^{-1})$, $s_2 = 10(g.L^{-1})$, $a = 0$.

number of degrees of freedom to the number of parameters of this distribution. The problem then is to know in which distribution we should restrict the search for the solution... To investigate this question, we run again the optimization procedure described previously but in limiting the number of freedom degrees for the parameters of a normal distribution. The results of 20 optimizations are plotted in Figure 5. Unfortunately, although the number of freedom degree is drastically reduced, the results indicate that the system might not be observable.

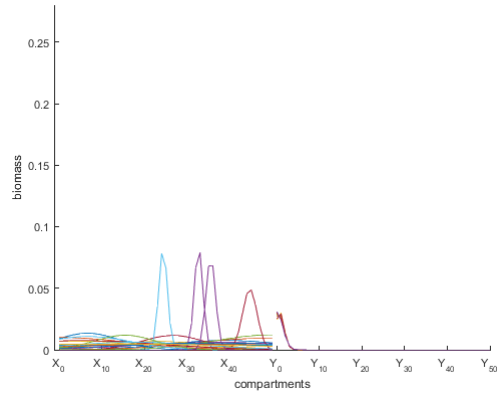


Fig. 5. Initial distributions obtained after using the least squared method on trajectories of total biomass and quantities of sugar, for $n_1 = \tilde{X} = 0.28 \times 0.75$, $n_2 = \tilde{Y} = 0.28 \times 0.25$, $s_1 = 10(g.L^{-1})$, $s_2 = 10(g.L^{-1})$, $a = 0$. The type of distribution is constrained to a normal form. 20 results are plotted.

A second idea is to ‘think practically’: in practice, prior to any experimental work, the biomass is prepared in specific conditions (cf. for instance Barthe et al. [2020]). The followed idea is to use the compartmental model as a virtual process to run simulations - several times - with arbitrary initial conditions on 10 g/L of glucose only. The final - very similar - distributions of biomass obtained under these conditions (starting from several random initial conditions) are plotted in Figure 6. Said otherwise, when the biomass is growing on glucose only,

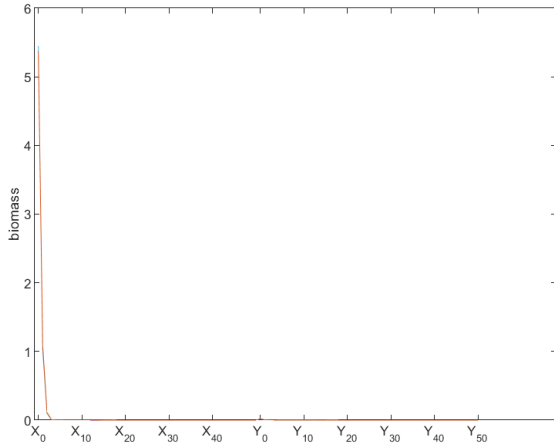


Fig. 6. Final distributions of biomass after growing on $10(g.L^{-1})$ glucose, starting with random initial distributions (50 repetitions)

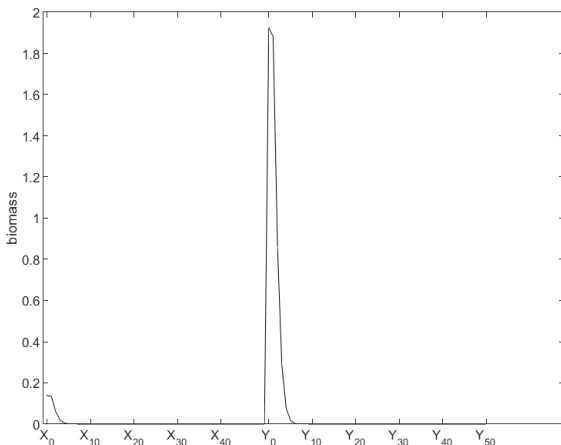


Fig. 7. Final distributions of biomass after growing on $10(g.L^{-1})$ of xylose starting with random initial distributions (50 repetitions)

the biomass compartments with a low number of XylR are attracting whatever the initial conditions are. Now, let us repeat this procedure but assuming there is only xylose in the medium. The results are now plotted in Figure 7. The compartments of both activated and inactivated biomasses with a low number of XylR are now attracting. In both cases, the final distributions obtained can obviously be approximated with a normal distribution in low XylR compartments of X and/or in Y .

Taking these results into account, we can further constraint the optimization algorithm and only consider that the compartments with low-XylR can be non-zero. If we retain only 3 or 4 first compartments, the number of parameters is not really more important than when considering parameters of the distributions. However, after several tests, it has not been possible to find only one set of initial conditions to explain the generated data. Thus, at present time, the observability problem of the compartmental model remains a key issue, to be investigated deeper in a coming work.

5. CONCLUSION

In this paper, we presented a new deterministic model of the diauxic growth observed in *E. coli* growing on glucose and xylose to find a possible mechanistic modeling of the lag phase duration. We compared its predictions to those obtained with another model that has been confronted to experimental data, and showed that they could give similar predictions of the lag phase duration. However, the lag time was sometimes different, highlighting a problem of unobservability. We have pursued several avenues, including the modifications of the model or the reduction of identified parameters, which unfortunately did not lead to the resolution of this problem which remains open at present time. Different techniques could be tested to free ourselves of the uniqueness of the solutions (set membership, multi-valued observers, change of coordinates...) as an alternative to reducing the model.

ACKNOWLEDGEMENTS

This work was supported by the 3BCAR Carnot (project HME) and the ANR (project JANUS; ANR-19-CE43-0004-01).

REFERENCES

- Barthe, M., Tchouanti, J., Gomes, P.H., Bideaux, C., Lestrade, D., Graham, C., Steyer, J.P., Méléard, S., Harmand, J., Gorret, N., Coccagn-Bousquet, M., and Enjalbert, B. (2020). Re-visiting diauxie: role of the molecular switch *xylR* in metabolic heterogeneity. *Embo Report*, 11(6), 1–16.
- Dedem, G.V. and Moo-Young, M. (1975). A model of diauxic growth. *Biotechnol. Bioeng.*, 17, 1301–1312.
- Graham, C., Harmand, J., Méléard, S., and Tchouanti, J. (2020). Bacterial metabolic heterogeneity: from stochastic to deterministic models. *AIMS*.
- Laikova, O., Mironov, A., and Gelfand, M. (2001). Computational analysis of the transcriptional regulation of pentose utilization systems in the gamma subdivision of proteobacteria. *FEMS Microbiol Lett*, 205, 315–322.
- Liquori, A.M., Monroy, A., Parisi, E., and Tripiciano, A. (1981). A theoretical equation for diauxic growth and its application to the kinetics of the early development of the sea urchin embryo. *Differentiation*, 20, 174–175.
- Monod, J. (1942). Recherches sur la croissance des cultures bactériennes. *Hermann Cie, Paris*.
- Schmidt, A., Kochanowski, K., Vedelaar, S., Ahrné, E., Volkmer, B., Callipo, L., Knoops, K., Bauer, M., Aebersold, R., and Heinemann, M. (2016). The quantitative and condition-dependent *Escherichia coli* proteome. *Nat Biotechnol*, 34, 104–110.
- Song, S. and Park, C. (1997). Organization and regulation of the d-xylose operons in *Escherichia coli* K-12: XylR acts as a transcriptional activator. *J Bacteriol*, 179, 7025–7032.
- Turon, V. (2015). Coupling dark fermentation with microalgal heterotrophy: Influence of fermentation metabolites mixtures, light, temperature and fermentation bacteria on microalgae growth. *Ph.D thesis, Université de Montpellier*.